*Published in : Biochimie (2008), vol. 90, pp. 1207-1223*
*Status : Postprint (Author's version)*

# Ligands playing musical chairs with G-quadruplex DNA: A rapid and simple displacement assay for identifying selective G-quadruplex binders

D. Monchaud [a], C. Allain [a] H. Bertrand [a], N. Smargiasso [b], F. Rosu [b], V. Gabelica [b], A. De Cian [c,d], J.-L. Mergny [c,d], M.-P. Teulade-Fichou [a,]

[a.] *Institut Curie, Section Recherche, CNRS UMR176, Centre Universitaire Paris XI, Bat. 110, 91405 Orsay, France*

[b.] *Laboratoire de Spectrométrie de Masse, GIGA-R, Université de Liège, Institut de Chimie Bat. B6c, B-4000 Liege, Belgium*

[c] *INSERM, U565, Acides Nucléiques: Dynamique, Ciblage et Fonctions Biologiques, Museum National d'histoire Naturelle USM 503, 43, Rue Cuvier, 75005 Paris, France*

[d.] *CNRS, UMR5153, Laboratoire des Régulations et Dynamique du Génome, Muséum National d'histoire Naturelle USM 503, 43, Rue Cuvier, 75005 Paris, France*

**Abstract**

We report here the details of G4-FID (G-quadruplex fluorescent intercalator displacement), a simple method aiming at evaluating quadruplex-DNA binding affinity and quadruplex- over duplex-DNA selectivity of putative ligands. This assay is based on the loss of fluorescence upon displacement of thiazole orange from quadruplex- and duplex-DNA matrices. The original protocol was tested using various quadruplex-and duplex-DNA targets, and with a wide panel of G-quadruplex ligands belonging to different families (i.e. from quinacridines to metallo-organic ligands) likely to display various binding modes. The reliability of the assay is further supported by comparisons with FRET-melting and ESI-MS assays.

**Keywords:** G-quadruplex DNA; Thiazole orange; G-quadruplex ligands; Fluorescent intercalator displacement

## 1. Introduction

The past few years have seen considerable efforts for designing and synthesizing novel compounds able to target G-quadruplex-DNA efficiently [1-5]. This unprecedented impetus originates in a growing body of evidence that bolsters G-quadruplex structures as pivotal elements to control cancer cell proliferation [6-15]. Such an exponential development requires powerful tools to select the best candidates based on rapid evaluation of quadruplex-DNA affinity and quadruplex- over duplex-DNA selectivity. To be effective, screening for selectivity has to be performed at the early stage of development and ideally this should be rapid and easy to implement. Currently several methods are employed, such as FRET-melting assay [16,17], SPR technique [18-20], ESI-MS analysis [21-24], fluorimetric titration [25,26] or equilibrium microdialysis [27-29]. Although these tests are reliable and powerful, they require specific equipments or buffer conditions, modified or immobilized oligonucleotides, and/or specific ligand properties (e.g. fluorescence). The recently described exonuclease I hydrolysis assay [30] is also promising, but requires a practical know-how which is not compatible with routine application, and is restricted to evaluate quadruplex- vs. single-stranded DNA selectivity.

We recently reported a Fluorescent Intercalator Displacement (G4-FID) assay [31], based on the displacement by ligands of the fluorescent probe thiazole orange (TO) from quadruplex- and duplex-DNA matrices. This test allows a convenient ranking of putative ligands as a function of their quadruplex-DNA affinities and their quadruplex- over duplex-DNA selectivities. G4-FID is an easy-to-use test since it requires neither modified oligonucleotides nor specific equipments. Initially, this assay was described with 22AG, a quadruplex-forming oligonucleotide (QFO) that mimics the human-telomeric sequence ([5'-$AG_3(T_2AG_3)_3$-3']). The choice of 22AG was fully justified by the obvious biological implications of telomeric quadruplexes but also because the folding of this sequence into quadruplex structure was thoroughly characterized [1,2,32,33]. However, the high polymorphism of telomeric quadruplex-DNA raises many questions and uncertainties with regard to ligand accommodation. In order to gain deeper insight into the sensitivity of our test to the targeted quadruplex structure, we examine here 22AG in different salt conditions. In addition, we tested another quadruplex structure

that is not subjected to structural interconversion, the TBA (thrombin binding aptamer) [34,35]. Finally, because quadruplex- vs. duplex-selectivity is a critical issue and because binding of both probe and ligand to duplex-DNA may be length- and sequence-dependent, we compare the results obtained with the 17-base pair duplex-DNA (dsl7) used in our initial work with a 26-bp duplex (ds26). G4-FID experiments reported herein were carried out with a set of 16 quadru-plex-ligands (from bisquinolinium to metallo-organic ligands) with two different QFOs (22AG [32,33], TBA [34,35]), in two different salt conditions ($Na^+$, $K^+$) and with two different DNA control duplex-DNAs (dsl7 [31] and ds26 [17]).

## 2. Material and methods

### *2.1. Material*

**MMQs, 360A, Phen-DC, Bipy-DC** and metallo-organic complexes **Pt-ttpy, Pt-ctpy, Cu-ttpy** and **Cu-ctpy** have been synthesized as previously described (see text for references). Stock solutions of these ligands (500 µM in DMSO) are used for G4-FID assay, unless otherwise stated, and are stored at -20 °C. TO was purchased from Aldrich and used without further purification. Oligonucleotides were purchased from Eurogentec (Belgium). 22AG is an oligonucleotide mimicking the human telomeric repeat: [5'-AG3($T_2$AG3)3-3']. The thrombin binding aptamer sequence (TBA) is: [5'-G2$T_2$G2TGTG2 $T_2$G2-3']. The 17 bp duplex is a biological sequence used in previous studies [31]; the sequences of the two complementary strands are the following: [5'-CCAGTTCGTAGTAACCC-3']/ [5'-GGGTTACTACGAACTGG-3']. The sequence of ds26 and ds12 are self-complementary [5'-C$A_2$TCG2ATCG$A_2$T2CG ATC$_2$GAT$_2$G-3'] and [5'-CGCG$A_2$T$_2$CGCG-3'], respectively. Fluorescence measurements are performed on a FluoroMax-3 spectrophotometer (Jobin-Yvon). UV-Vis measurements are performed on a Uvikon XL Secomam spectrophotometer.

### *2.2. Preparation of oligonucleotides*

Quadruplexes from 22AG and TBA are prepared by heating the corresponding oligonucleotides at 90 °C for 5 min in a 10 mM sodium cacodylate buffer pH 7.3, 100 mM KC1 and cooling in ice to favor the intramolecular folding by kinetic trapping. For 22AG in $Na^+$ buffer, the same protocol is applied in a 10 mM sodium cacodylate buffer pH 7.3, 100 mM NaCl. Duplex-DNAs are prepared by heating the two corresponding complementary strands (ds17) or the self-complementary strand (ds26 and dsl2) at 90 °C for 5 min in a 10 mM sodium cacodylate buffer pH 7.3, 100 mM KC1 followed by a slow cooling over 6 h. Concentrations are determined by UV-Vis measurements (after thermal denatur-ation, 5 min at 85 °C) at 260 nm before use.

### *2.3. Fluorimetric titration*

A temperature of 20 °C is kept constant with a thermostated cell holder. Each titration is performed in a 3-ml cell, in 10 mM sodium cacodylate buffer pH 7.3, 100 mM KC1 (22AG, TBA, dsl7 and ds26) or NaCl (22AG), in a total volume of 3 ml. Titrations are performed with the addition of TO (1.0 µM) followed by the addition of oligonucleotide (up to 15.0 µM), at 501 nm excitation wavelength, and data are collected between 510 and 750 nm (fluorescence area).

### *2.4. G4-FID protocol*

A temperature of 20 °C is kept constant with thermostated cell holders. Each experiment is performed in a 3-ml cell, in 10 mM sodium cacodylate buffer pH 7.3 with 100 mM KC1 or 100 mM NaCl depending on the experiments, in a total volume of 3 ml. The G4-FID assay is designed as follows: 0.25 µM pre-folded DNA target is mixed with thiazole orange (0.50 µM for 22AG, TBA and ds17, 0.75 µM for ds26). Each ligand addition step (from 0.5 to 10 equivalents) is followed by a 3-min equilibration period after which the fluorescence spectrum is recorded. The percentage of displacement is calculated from the fluorescence area (FA, 510-750 nm, $\lambda_{ex}$ = 501 nm), using: percentage of displacement = 100 - [(FA/$FA_0$) x 100], $FA_0$ being the fluorescence of TO bound to DNA without added ligand. The percentage of displacement is then plotted as a function of the concentration of added ligand.

### *2.5. ESI-MS protocol*

Electrospray mass spectrometry experiments are performed on a Micromass Q-TOF Ultima Global using the standard electrospray source. The samples containing the DNA-ligand mixtures are prepared in 80:20 or 85:15 (v/v) 150 mM ammonium acetate/methanol. The following tuning parameters are used: electrospray needle voltage = -2.2 kV (negative ion mode), cone voltage = 100 V, RF lens 1 is varied between 40 V and 100 V,

collision energy = 10 V, source pressure = 4.0 mbar. The relative concentrations of free DNA and complexes are calculated from the peak areas and the total DNA concentration using Eq. (1), where *n* is the number of bound ligands (0:1 corresponds to the free DNA). $[DNA]_0$ is here in all cases equal to 5 µM. The concentration of bound ligand is calculated from the concentrations of complexes using Eq. (2), and the concentration of free ligand is calculated by difference (Eq. (3)). The values reported here are the mean values calculated over several RF lens 1 voltages and several charge states.

$$[n:1] = [\mathrm{DNA}]_0 \cdot \frac{A_{(n:1)}}{\sum_{n=0}^{3} A_{(n:1)}} \quad (1)$$

$$[\mathrm{L}]_{\mathrm{bound}} = \sum_{n=1}^{3} n \cdot [n:1] \quad (2)$$

$$[\mathrm{L}]_{\mathrm{free}} = [\mathrm{L}]_0 - [\mathrm{L}]_{\mathrm{bound}} \quad (3)$$

## 3. Results

### *3.1. Thiazole orange association with oligonucleotides*

TO (Fig. 1A) is a particularly interesting DNA fluorescent probe because its fluorescence quantum yield ($\Phi_F$) is very low when free in solution ($\Phi_F = 2 \times 10^{-4}$), and is enhanced by a factor of 500 to 1000 when bound to DNA [36]. Furthermore, TO does not exhibit marked selectivity for diverse DNA structures (e.g. duplex- or quadruplex-DNA) [36]. This poor selectivity allows comparing the competitive displacement of the bound probe by ligands regardless of the nature of the DNA. As this is a key point to validate our approach, we investigated thiazole orange association with DNA in more detail. First a series of fluorimetric titrations was performed with TO, and two intramolecular quadruplexes 22AG and TBA (Fig. 1). Then comparison was drawn with two tetramolecular quadruplexes ($[5'\text{-}TG_3T\text{-}3']_4$ and $[5'\text{-}TG_4T\text{-}3']_4$, respectively named hereafter $TG_3T$ and $_{TG4T}$, see Supplementary Material). Finally, the two control duplex-DNAs differing in sequence and length i.e. ds17 and ds26 were investigated (Fig. 2).

As seen in Figs. 1 and 2, TO binds all the studied structures with similar apparent affinity per site ($K_a$/site from 2 to 3 x $10^6$ $M^{-1}$). The main difference stands in the stoichiometry of the TO/DNA association: in the case of intramolecular quadruplexes (22AG and TBA, Fig 1), processing the data by least-square fitting procedure evidenced the formation of a 1:1 complex. These observations, consistent with the asymmetrical nature of the two external tetrads constitutive of intramolecular quadruplexes [1,2,32,33], were supported by Job plot analysis (Supplementary Material). Interestingly the study of TO binding with the two symmetrical tetramolecular quadruplexes $TG_3T$and $TG_4T$ evidenced a 2:1 TO/DNA association in both cases that was also supported by Job plot analysis (Supplementary Material). These results are in agreement with the structural equivalence of the two external tetrads in tetramolecular quadruplex structures. On the other hand, and unexpectedly, the increase in quantum yield of TO was much lower (~ 60-fold) in the presence of tetramolecular quadruplexes than in the presence of intramolecular quadruplexes (~ 400-fold for 22AG or TBA), thereby indicating the critical role of the loops and quartet surrounding in the immobilization of the probe. However, a full understanding of this phenomenon would require more thorough photophysical investigations.

Similar experiments were then conducted with the short duplex-DNA (dsl7) and the longer one (ds26). They evidenced the formation of 2:1 and 3:1 complexes respectively (Fig. 2). The slight difference in the two fitting curves do not allow to firmly assess the formation of a unique species and it is likely that a mixture of both 2:1 and 3:1 species can be found in our experimental conditions. A higher amount of bound TO could have been expected with respect to previous studies that reported for ~ 3 TO binding sites for a 8 bp hairpin duplex-DNA sequence [37], but complexes of higher order (>3:1) seem to be excluded herein, even with the longest duplex-DNA ds26. This could be explained by the rather low concentration used in the experiment as compared to the affinity/site (1 order of magnitude lower than $K_d$) and/or to the existence of site(s) of lower affinity. Also sensitivity of TO to sequence characteristics could be involved.

*Published in : Biochimie (2008), vol. 90, pp. 1207-1223*
*Status : Postprint (Author's version)*

***Fig. 1.*** *Fluorimetric titrations of TO (1 µM) with 22AG in 100 mM $K^+$ (A) and 100 mM $Na^+$ (B) and TBA (C) in 10 mM sodium cacodylate (pH 7.2) with 100 mM KC1 (A,C) or NaCl (B). Theoretical fitting curves (plain and dotted lines) are calculated with Specfit32 version 3.0 (Spectrum Software Associates, Marlborough, MA, USA).*

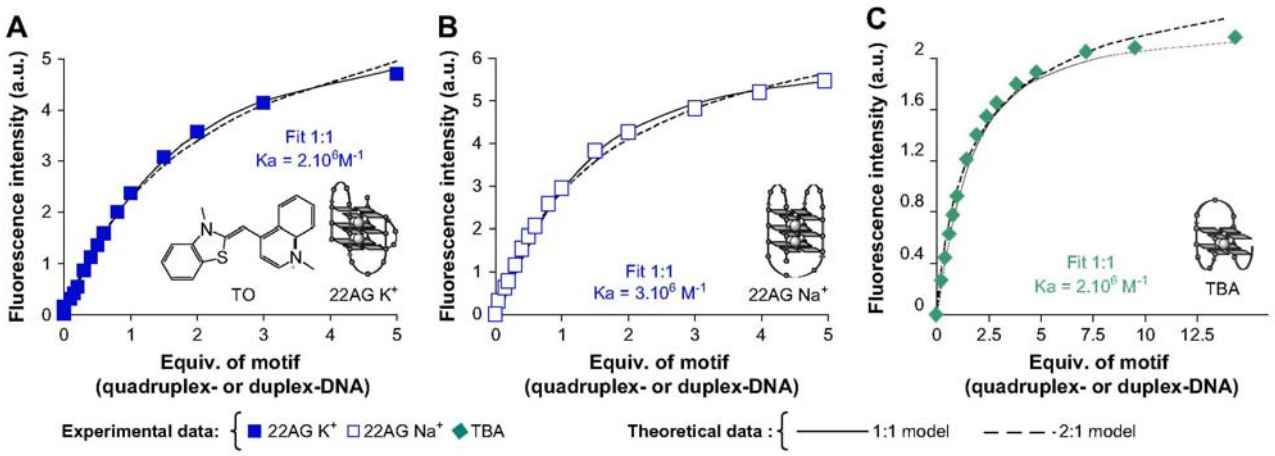


***Fig. 2****. Fluorimetric titrations of TO with dsl7 (A) and ds26 (B) in 10 mM sodium cacodylate (pH 7.2) with 100 mM KC1. Theoretical fitting curves (plain and dotted lines) are calculated with Specfit32 version 3.0 (Spectrum Software Associates).*

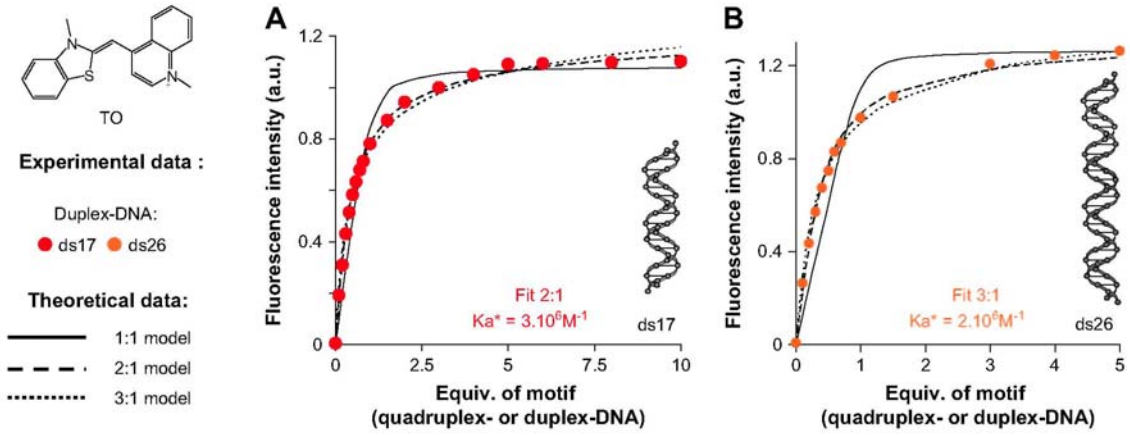


Fluorimetric titration enables a detection of major ligand— DNA complexes present in solution. To gain further insights into the TO/DNAs association stoichiometries, electrospray mass spectrometry (ESI-MS) analysis appeared the method of choice because it allows distinguishing all complexes present in solution by their mass [38] (see also companion paper by Rosu et al. in the same issue). However, a perfect agreement when comparing results obtained by fluorescence and ESI-MS cannot be expected due to the differences in conditions of both methods [38]. ESI-MS spectra obtained when TO is mixed with duplex DNA ds17 (Fig. 3A) and ds12 (Fig. 3B) show the statistical formation of 1:1, 2:1, and 3:1 complexes, the latter being very weakly abundant. A similar ESI-MS profile was obtained with ds26 but with a higher proportion of 3:1 complex (not shown). The amount of 3:1 complex is directly correlated with the size of the duplex. The stoichiometries found by ESI-MS confirm the findings from fluorescence titration data.

The association of TO with quadruplex-DNA was also monitored by ESI-MS. Results obtained with TBA and Telo3.5 ([5'-$G_3(T_2AG_3)_3$-3'] that differs from 22AG by only 1 nucleotide) are shown in Fig. 3C and D, respectively. In both cases the 1:1 ligand-DNA complex is the major species. The 2:1 complex is marginal with TBA, in agreement with fluorescence titration. However, two other binding sites are found with Telo3.5. The contribution of the 2:1 and 3:1 complexes was not evidenced by fluorimetric titrations. This may be due either to the lower concentrations used in fluorescence titration, or to different TO fluorescence quantum yields for the

different binding sites. ESI-MS data also evidence a lower binding affinity of TO for TBA, which was also not detected by the fluorimetric titration (although a lower $\Phi_F$ could be noticed). Thus, the less specific interaction of TO with telomeric quadruplex, added of its lower affinity for TBA, were underestimated by fluorimetric titrations, reminiscent of what it is usually observed when comparing fluorescence and ESI-MS results [38]. These observations are of importance to interpret probe displacement by ligands and will be discussed further in the light of G4-FID results. Altogether, our results underline the difficulties in accurately determining DNA-ligand affinity constants, pointing out the need for comparing data obtained with various techniques.

Based on the results of the above experiments, the competitive displacement by ligands was achieved at 2:1 (for 22AG, TBA and ds17) and 3:1 (for ds26) TO/oligonucleotide ratio, likely to favor the occupation of one (22AG, TBA and ds17) and two (ds26) binding sites, thereby limiting the existence of mixtures of complexes in solution. These conditions were also fixed with respect to preliminary FID assays conducted at various probe/DNA ratios which led to similar FID results [31].

***Fig. 3**. ESI-MS profile of the association of TO with dsl7 (A), ds12 (B), TBA (C) and 22AG (D), obtained with 5 µM of DNA and 10 µM of TO, in 150 mM ammonium acetate, 15% MeOH.*

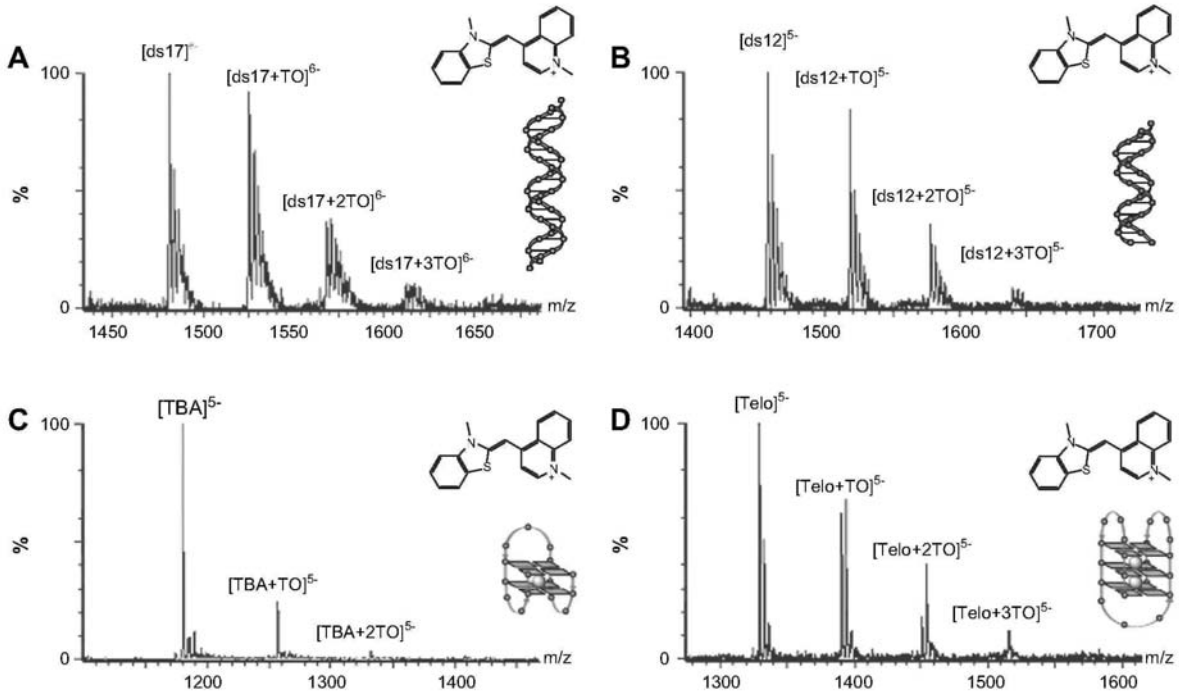


*3.2. G4-quadruplex ligands and G4-FID results*

To evaluate the impact of quadruplex- and duplex-DNA modification on G4-FID results, a set of 16 recently reported ligands of clearly distinct nature was studied (Fig. 4): 4 quinacridines ($MMQ_1$, $MMQ_3$, $MMQ_{10}$ and $MMQ_{12}$) [25,26,39,40], 3 W-methylated quinacridines ($MMQ_{15}$, $MMQ_{16}$ and $MMQ_{18}$) [39], 5 bisquinolinium derivatives (360A [41-46], **Phen-DC$_3$, Phen-DC$_6$, Bipy-DC$_3$** and **Bipy-DC$_6$** [45,46]) and 4 metallo-organic complexes **(Pt-ttpy, Pt-ctpy, Cu-ttpy** and **Cu-ctpy)** [47]. For each ligand, a series of FID experiments was performed with four different DNA targets (22AG in $K^+$ or $Na^+$ condition, TBA, ds17 and ds26) and the DNA affinity was evaluated by the concentration required to decrease the fluorescence of the probe by 50%, reflecting binding to quadruplex- ($^{G4}DC_{50}$) or to duplex-DNA ($^{ds}DC_{50}$). Comparison of $^{G4}DC_{50}$ and $^{ds}DC_{50}$ values thus provides a global "mapping" of the interaction of a given ligand with the diverse DNA forms. Results obtained with $MMQ_{16}$ were selected as a representative example and are shown in Fig. 5.

FRET-melting assays showed that $MMQ_{16}$ is a particularly efficient ($\Delta\Gamma 1/2$ = 16 °C) and selective G-quadruplex ligand [39]. In the G4-FID assay, $MMQ_{16}$ indeed exhibits a high TO displacement ability from quadruplex-DNA,

with $^{G4}DC_{50}$ values in the submicromolar range (from 0.11 to 0.14 µM, Fig. 5) regardless of the nature of the quadruplex-DNA used. From a selectivity point of view, the binding of $MMQ_{16}$ to duplex-DNA seems slightly dependent on the duplex-DNA characteristics (length and sequence) since $^{ds}DC_{50}$ values of >2.5 and 1.9 µM were observed for ds17 and ds26, respectively (Fig. 5). In the case of ds26, the ratio of $^{ds}$DC5o and $^{G4}$DC50 values enables an easy estimation of $MMQ_{16}$ selectivity for quadruplex- over duplex-DNA: this selectivity ($^{ds}DC_{50}$/ $^{G4}DC_{50}$) ranges from 13 (22AG $K^+$, Fig. 5) to 17 (22AG $Na^+$, Fig. 5).

In the present case, the displacement of TO from ds17 was slightly more difficult than with ds26, and the 50% threshold was not reached; the selectivity was then not evaluated by the $^{ds}DC_{50}/^{G4}DC_{50}$ ratio as it requires an unreliable extrapolation of the curve to higher concentrations. As our goal here is to confirm that selectivity ranking does not depend on the nature of the duplex-DNA (e.g. on its length), results obtained with ds17 and ds26 have to be compared in each situation; therefore, each time the ligand has a poor TO displacement ability (as it is the case with $MMQ_{16}$ and ds17) we defined an estimated selectivity (Est. Sel.) as follows [31]: (1) the value $^{ds}D_{(2.5\mu M)}$, i.e. the TO-displace-ment induced by the presence of 2.5 µM of ligand (herein, $^{ds}D_{(2.5\mu M)}$ = 43.2%, Fig. 5), is determined; (2) the concentration of ligand required to reach the same level of TO-displacement on G-quadruplex DNA, defined as $^{G4}C$, is measured. Herein, $^{G4}C$ = 0.09, 0.10 and 0.11 µM for 22AG $Na^+$, TBA and 22AG $K^+$ respectively; (3) the estimated selectivity is established according to the following ratio: Est. Sel. = $2.5/^{G4}C$, which leads to an estimated selectivity of 28, 25 and 23 for 22AG $Na^+$, TBA and 22AG $K^+$, respectively.

The same set of experiments and data treatments were then carried out with the above-mentioned series of ligands. $^{G4}DC_{50}$ and $^{ds}DC_{50}$ values measured for all ligands are compiled in Tables 1-4, as well as the selectivity ratios ($^{ds}DC_{50}$/ $^{G4}DC_{50}$) and the estimated selectivity (Est. Sel.). These values are also represented as bar graphs to ensure a global overview of the TO displacement ability (Fig. 6) and quadruplex- over duplex-DNA selectivity (Fig. 7), as well as the FRET-melting results (Fig. 8) of all the series tested.

### *3.3. G4-FID results of quinacridines ($MMQ_1$, $MMQ_3$, $MMQ_{10}$ and $MMQ_{12}$)*

Quinacridines are moderate ($MMQ_1$, $DC_{50}$ between >2.5 and 1.14 µM, Table 1, Fig. 6) to strong TO-displacers ($MMQ_3$ to $MMQ_{12}$, $^{G4}DC_{50}$ down to 0.09 µM, Table 1, Fig. 6) when quadruplex-DNA was targeted. Most importantly, this ability shows a limited dependence on the nature of the quadruplex-matrix used, with, in most cases, an easier displacement from TBA than 22AG ($^{G4}DC_{50}$(TBA) < $^{G4}$D-$C_{50}$(22AG), Table 1, Fig. 6). It is nevertheless interesting to note that $MMQ_1$ displaces TO from TBA whereas it is shown to be very poorly active on 22AG. The difference in G4-FID responses observed with 22AG and TBA might either result from a higher accessibility of quartets on TBA or stronger interaction with specific elements such as loops or grooves of TBA, or might indicate that $MMQ_1$ binds to secondary sites on 22AG before (or instead of) displacing the probe. This is consistent with previous SPR measurements evidencing that 22AG can accommodate 3-4 molecules of $MMQ_1$ (with a rather low $K_a$ value of 8.6 x $10^5$ $M^{-1}$ [26]), also observed by ESI-MS analysis (not shown), thereby leading to a mostly indirect competition with TO bound to 22AG. We can also speculate that, as has been pointed out by ESI-MS analysis (Fig. 3), the displacement of TO from TBA is easier thanks to a weaker affinity of the probe for this quadruplex, as compared to 22AG. In this regard, and although the $MMQ_1$ example points out to the limitations of the present assay, the comparison of the two matrices may give interesting clues to quartet vs. secondary site occupancy by ligands.

The TO-displacing ability seems in direct correlation with the number of positive charges of the ligands (from 2 to 6 in the conditions of the test): the highly cationic molecules are the most efficient TO-displacers ( $^{G4}$DC50 down to 0.09 µM with $MMQ_{12}$, bearing 6 positive charges, Table 1, Fig. 6). This trend is also observed with the two duplex-DNAs. These results underline that this series is very moderately selective, with $^{ds}DC_{50}$/ $^{G4}DC_{50}$ ratio (or Est. Sel.) comprised between 0.3 and 5.7 (Table 1, Fig. 7). As expected an increase in the cationic charge of the ligand is detrimental for the quadruplex-over duplex-DNA selectivity. This observation is assumed to originate in the electrostatically-driven random surface interactions with duplex-DNA.

Similar trends have already been observed through the FRET-melting assay, since compounds of high cationic charge exhibited high $\Delta T_{1/2}$ value (from 12.5 to 30 °C from $MMQ_1$ to $MMQ_{12}$ respectively, Table 1, Fig. 8) [39]. On the other hand, in terms of selectivity, the G4-FID trend is confirmed. Indeed, the quadruplex- vs. duplex-selectivity of a compound is estimated with the *S* value (De Cian et al., in preparation), defined as the ratio between the $\Delta T_{1/2}$ values in the presence and in the absence of the duplex competitor (3 µM), following the equation: $S = \Delta T_{1/2}(+ds26)/\Delta T_{1/2}(-ds26)$. Thus, *S* reflects the preferential binding of a compound to the quadruplex-DNA ($S \rightarrow 1$) or to the duplex-DNA ($S \rightarrow 0$). Herein, $MMQ_1$ and $MMQ_3$ were found to be moderately selective *(S* up to 0.38), while **$MMQ_{10}$** and **$MMQ_{12}$** were non-selective *(S* down to 0.05).

*Published in : Biochimie (2008), vol. 90, pp. 1207-1223*
*Status : Postprint (Author's version)*

***Table 1** : Comparative G4-FID results for quinacridines*

| | | | $MMQ_1$ | $MMQ_3$ | $MMQ_{10}$ | $MMQ_{12}$ |
|---|---|---|---|---|---|---|
| Duplex-DNA | dsl7 | $^{ds}DC_{50}$ (µM) | >2.5 | 0.67 | 0.50 | 0.40 |
| | ds26 | $^{ds}DC_{50}$ (µM) | >2.5 | 0.86 | 0.55 | 0.52 |
| Quadruplex-DNA | 22AG K+ | $^{G4}DC_{50}$ (µM) | >2.5 | 1.18 | 0.61 | 0.48 |
| | | Sel.[a] vs. dsl7 | 0.3[b] | 0.6 | 0.8 | 0.8 |
| | | Sel.[a] vs. ds26 | 0.4[b] | 0.7 | 0.9 | 1.1 |
| | $22AGNa^+$ | $^{G4}DC_{50}$ (µM) | >2.5 | 0.90 | 0.41 | 0.14 |
| | | Sel.[a] vs. dsl7 | 0.6[b] | 0.7 | 1.2 | 2.8 |
| | | Sel.[a] vs. ds26 | 0.6[b] | 0.9 | 1.3 | 3.7 |
| | TBA | $^{G4}$DC50 (µM) | 1.14 | 0.22 | 0.16 | 0.09 |
| | | Sel.[a] vs. dsl7 | 3.5[b] | 3.0 | 3.1 | 4.4 |
| | | Sel.[a] vs. ds26 | 3.8[b] | 3.9 | 3.4 | 5.7 |
| FRET-melting assay | $\Delta T_{1/2}$ (°C) | | 12.5 | 19.7 | 21.0 | 30.0 |
| | $\Delta T_{1/2}$ with 3 µM ds26 (°C) | | 4.5 | 7.6 | 1.1 | 9.7 |
| | $\Delta T$ with 10 µM ds26 (°C) | | 1.1 | 5.6 | 0.1 | 4.8 |

[a] Sel. stands for G4-FID selectivity, defined as $^{ds}DC_{50}/^{G4}DO_{50}$ ratio.
[b] In the case of $^{ds}DC_{50}$>2.5 µM, the selectivity is estimated on the basis of TO displacement (%) obtained with 2.5 µM of ligand with ds26 and the concentration required with 22AG to reach the same displacement ($^{G4}$C): Sel. = 2.5/$^{G}$ C. Experimental errors are estimated at ± 5% for G4-FID assay and ±1 °C for FRET-melting assay.

***Table 2:** Comparative G4-FID results for N-methylated quinacridines*

| | | | $MMQ_{15}$ | $MMQ_{16}$ | $MMQ_{18}$ |
|---|---|---|---|---|---|
| Duplex-DNA | dsl7 | $^{ds}DC_{50}$ (µM) | 0.92 | >2.5 | 0.39 |
| | ds26 | $^{ds}DC_{50}$ (µM) | 1.61 | 1.89 | 0.45 |
| Quadruplex-DNA | 22AG $K^+$ | $^{G4}DC_{50}$ (µM) | 0.22 | 0.14 | 0.16 |
| | | Sel.[a] vs. dsl7 | 4.2 | 22.7[b] | 2.4 |
| | | Sel.[a] vs. ds 26 | 7.3 | 13.5 | 2.8 |
| | 22AG $Na^+$ | $^{G4}DC_{50}$ (µM) | 0.39 | 0.11 | 0.11 |
| | | Sel.[a] vs. dsl7 | 2.3 | 27.7[b] | 3.3 |
| | | Sel.[a] vs. ds26 | 4.1 | 17.2 | 4.1 |
| | TBA | $^{G4}DC_{50}$ (µM) | 0.36 | 0.12 | 0.11 |
| | | Sel.[a] vs. dsl7 | 2.5 | 25.0[b] | 3.3 |
| | | Sel.[a] vs. ds26 | 4.5 | 15.7 | 4.1 |
| FRET-melting assay | $\Delta T_{1/2}$(°C) | | 9.5 | 16.0 | 21.5 |
| | $\Delta T_{1/2}$ with 3 µM ds26 (°C) | | 3.0 | 9.3 | 8.3 |
| | $\Delta T_{1/2}$with 10 µM ds26 (°C) | | - | 3 | 4.1 |

[a] Sel. stands for G4-FID selectivity, defined as $^{ds}DC_{50}/^{G4}DC_{50}$ ratio.
[b] In the case of $^{ds}DC_{50}$>2.5 µM, the selectivity is estimated on the basis of TO displacement (%) obtained with 2.5 µM of ligand with ds26 and the concentration required with 22AG to reach the same displacement ($^{G4}$C): Sel. = 2.5:$^{G4}$C. Experimental errors are estimated at ± 5% for G4-FID assay and ±1 °C for FRET-melting assay.

*Published in : Biochimie (2008), vol. 90, pp. 1207-1223*
*Status : Postprint (Author's version)*

***Table 3:*** *Comparative G4-FID results for bisquinolinium compounds*

| | | | 360A | Phen-$DC_3$ | Phen-$DC_6$ | Bipy-$DC_3$ | Bipy-$DC_3$ |
|---|---|---|---|---|---|---|---|
| Duplex-DNA | dsl7 | $^{ds}DC_{50}$ (μM) | >2.5 | >2.5 | >2.5 | >2.5 | >2.5 |
| | ds26 | $^{ds}DC_{50}$ (μM) | >2.5 | >2.5 | >2.5 | >2.5 | >2.5 |
| Quadruplex-DNA | 22AG $K^+$ | $^{G4}DC_{50}$ (μM) | 0.32 | 0.31 | 0.57 | 0.40 | 0.63 |
| | | Sel.[a] vs. dsl7 | 41.6[b] | 10.9[b] | 11.4[b] | 12.5[b] | 7.3[b] |
| | | Sel.[a] vs. ds26 | 35.7[b] | 20.8[b] | 13.1[b] | 15.2[b] | 12.5[b] |
| | 22AG $Na^+$ | $^{G4}DC_{50}$ (μM) | 0.29 | 0.25 | 0.52 | 0.57 | 0.69 |
| | | Sel.[a] vs. dsl7 | 50.0[b] | 13.8[b] | 13.1[b] | 6.1[b] | 5.7[b] |
| | | Sel.[a] vs. ds26 | 41.6[b] | 25.0 | 15.2[b] | 7.5[b] | 8.6[b] |
| | TBA | $^{G4}DC_{50}$ (μM) | 0.44 | 0.30 | 0.44 | 0.74 | 0.79 |
| | | Sel.[a] vs. dsl7 | 31.2[b] | 13.9[b] | 14.7[b] | 5.1[b] | 5.7[b] |
| | | Sel.[a] vs. ds26 | 25.0[b] | 25. l[b] | 17.9[b] | 6.6[b] | 9.2[b] |
| FRET-melting assay | $\Delta T_{1/2}$ (°C) | | 25.1 | 29.7 | 28.5 | 15.2 | 9.6 |
| | $\Delta T_{1/2}$ with 3 μM ds26 (°C) | | 22.5 | 27.9 | 29.0 | 12.9 | 8.3 |
| | $\Delta T$i/2 with 10 μM ds26 (°C) | | 21.7 | 26.2 | 26.6 | 10.8 | 6.2 |

[a] Sel. stands for G4-FID selectivity, defined as $^{ds}DC_{50}/^{G4}DC_{50}$ ratio.
[b] In the case of $^{ds}DC_{50}$>2.5 μM, the selectivity is estimated on the basis of TO displacement (%) obtained with 2.5 μM of ligand with ds26 and the concentration required with 22AG to reach the same displacement ($^{G4}C$): Sel. = 2.5/$^{G4}C$. Experimental errors are estimated at ± 5% for G4-FID assay ±1 °C for FRET-melting assay.

***Table 4****: Comparative G4-FID results for metallo-organic compounds*

| | | | Pt-ttpy | Pt-ctpy | Cu-ttpy | Cu-ctpy |
|---|---|---|---|---|---|---|
| Duplex-DNA | dsl7 | $^{ds}DC_{50}$ (μM) | 1.26 | 0.86 | >2.5 | >2.5 |
| | ds26 | $^{ds}DC_{50}$ (μM) | 1.92 | 1.37 | >2.5 | >2.5 |
| Quadruplex-DNA | 22AG $K^+$ | $^{G4}DC_{50}$ (μM) | 0.18 | 0.25 | 0.30 | 0.19 |
| | | Sel.[a] vs. dsl7 | 7.0 | 3.4 | 22.7[b] | 15.6[b] |
| | | Sel.[a] vs. ds26 | 9.6 | 5.5 | 41.6[b] | 19.3[b] |
| | 22AG$Na^+$ | $^{G4}DC_{50}$ (μM) | 0.17 | 0.39 | 0.34 | 0.33 |
| | | Sel.[a] vs. dsl7 | 7.4 | 2.2 | 20.8[b] | 8.9[b] |
| | | Sel.[a] vs. ds26 | 10.2 | 3.5 | 35.7[b] | 11.4[b] |
| | TBA | $^{G4}DC_{50}$ (μM) | 0.14 | 0.19 | 0.53 | 0.21 |
| | | Sel.[a] vs. dsl7 | 9.0 | 4.5 | 13.1[b] | 13.9[b] |
| | | Sel.[a] vs. ds26 | 12.4 | 7.2 | 27.8[b] | 16.6[b] |
| FRET-melting assay | $\Delta T_{1/2}$ (°C) | | 11.3 | 16.2 | 15.3 | 10.0 |
| | $\Delta T_{1/2}$ with 3 μM ds26 (°C) | | 9.1 | 10.2 | 14.6 | 8.5 |
| | $\Delta T$i/2 with 10 μM ds26 (°C) | | 6.4 | 6.0 | 13.5 | 4.8 |

[a] Sel. stands for G4-FID selectivity, defined as $^{ds}DC_{50}/^{G4}DC_{50}$ ratio.
[b] In the case of $^{ds}DC_{50}$>2.5 μM, the selectivity is estimated on the basis of TO displacement (%) obtained with 2.5 μM of ligand with ds26 and the concentration required with 22AG to reach the same displacement ($^{G4}C$): Sel. = 2.5/$^{G4}C$. Experimental errors are estimated at ± 5% for G4-FID assay and ±1 °C for FRET-melting assay.

***Fig. 4.*** *Structures of quinacridines ($MMQ_1$, $MMQ_3$, $MMQ_{10}$ and $MMQ_{12}$), N-methylated quinacridines ($MMQ_{15}$, $MMQ_{16}$ and $MMQ_{18}$), bisquinolinium* ***(360A, Phen-DC$_3$, Phen-DC$_6$, Bipy-DC$_3$*** *and* ***Bipy-DC$_6$)*** *and metallo-organic* ***(Pt-ttpy, Pt-ctpy, Cu-ttpy*** *and* ***Cu-ctpy)*** *ligands evaluated through G4-FID assay.*

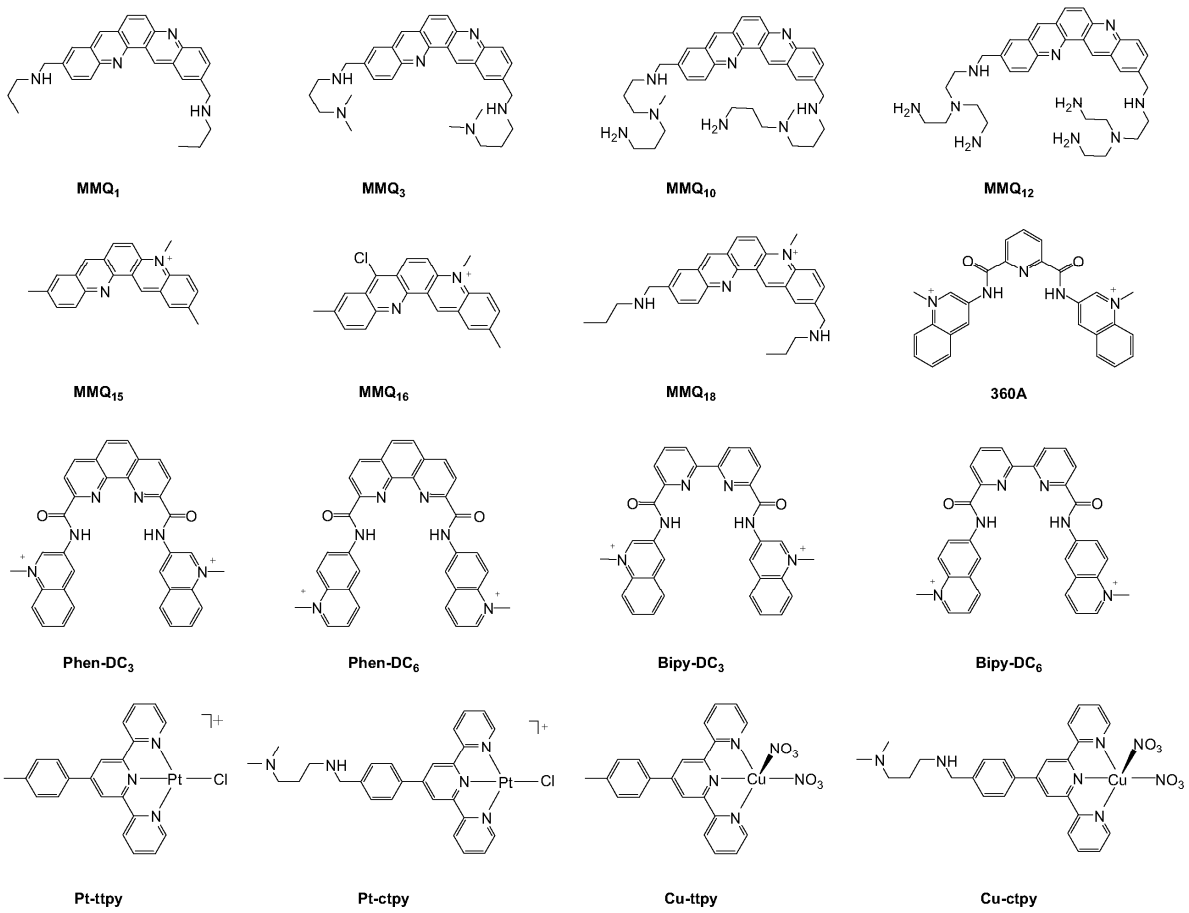


*3.4. G4-FID results of N-methylated quinacridines ($MMQi_5$, $MMQ_{16}$ and $MMQ_{18}$)*

As compared with the parent quinacridine series, Λ7-methylated quinacridines (Fig. 4) [39] have improved quad-ruplex-interaction properties that may originate in improved PI-stacking interactions with the external G-quartet(s) of the quadruplex structure. This improvement is due to the decrease of the electronic density of the central aromatic core of the ligand through quaternarization of one of the intracyclic nitrogen atoms [39]. In the present assay, **$MMQ_{16}$** and **$MMQ_{18}$** are more potent TO-displacers from quadruplex-DNA ($0.11 < {}^{G4}DC_{50} < 0.16$ µM, Table 2, Figs. 5 and 6) than **$MMQ_{15}$** ($0.22 < {}^{G4}DC_{50} < 0.39$ µM, Table 2, Fig. 6). Remarkably, in terms of selectivity, **$MMQ_{16}$** offers the best results ($13 <$ G4-FID Sel. $< 28$, Table 2, Figs. 5 and 7) as compared to **$MMQ_{15}$** or **$MMQ_{18}$** (${}^{ds}DC_{50}/{}^{G4}DC_{50} < 7$, Table 2, Fig. 7).

Again, this trend is consistent with affinity and selectivity obtained via the FRET-melting assay [39]: the triscationic **$MMQ_{18}$** display a significant higher $\Delta T_{1/2}$ value than monoca-tionic $MMQ_{15}$ (21.5 vs. 9.5 °C, Table 2, Fig. 8), whereas an inverse correlation was observed between selectivity and the cationic charge of the ligand ($0.58 < S < 0.31$ from $MMQ_{15} \approx MMQ_{16}(1+)$ to $MMQ_{18}(3+)$, Table 2). Altogether the data show that $MMQ_{16}$ offers the best compromise evidently due to electronic and steric effects of the chloride atom, which increases Π-stacking while hampering insertion between base-pairs. These results definitely pinpoint the importance of molecular charge and electronic density, which should be properly balanced in order to improve the G-quadruplex specific recognition.

The specificity of $MMQ_{16}$ for G-quadruplex DNA was confirmed by ESI-MS analysis. As already reported [21-24,38], this technique allows to determine the amount of bound ligand to various DNA-structures, and hence it is a particularly powerful to gain insight into the affinity and selectivity for quadruplex- over duplex-DNA. Additionally, one of the great advantages of ESI-MS is to enable a direct read-out of the stoi-chiometry of the interaction. Experiments were carried out to determine the stoichiometry of association of $MMQ_{16}$ and $MMQ_{18}$ with quadruplex-DNA i.e. Telo4, [5'-$(T_2AG_3)_4$-3'] that differs from 22AG by only 2 nucleotides, and ds12. As seen in Fig. 9A and C, the ESI-MS analysis allows determination of the existence of a site of higher affinity for both ligands with quadruplex-DNA as well as a site of lower affinity, which corresponds to the two external tetrads of the quadruplex structure. Additionally, these results underlined that the fixation of $MMQ_{18}$ (6.3 µM) is higher than that of $MMQ_{16}$ (3.8 µM), which is consistent with G4-FID and FRET-melting results. Interestingly, when the same experiments were carried out with duplex-DNA, the fixation of $MMQ_{18}$ (6.1 µM) was also higher than the one of $MMQ_{16}$ (0.7 µM), which implies a low (6.3/6.1 ~ 1) and a high (3.8/0.7 = 5.4) quadruplex-selectivity of $MMQ_{18}$ and $MMQ_{16}$ respectively, again fully reminiscent of what has been observed with G4-FID and FRET-melting assays (Fig. 9B and D). Similar experiments were carried out with $MMQ_1$, $MMQ_3$, $MMQ_{10}$ and $MMQ_{12}$ (Supplementary Material), which support the overall agreement between both techniques.

***Fig. 5.*** *G4-FID mapping of $MMQ_{16}$, i.e. G4-FID curves obtained with TBA (black curve), 22AG in $Na^+$ (blue curve, white square) or $K^+$-rich buffer (blue curve and square) and the duplex-DNAs dsl7 (red curve) and ds26 (orange curve). Experimental conditions: [oligonucleotide] = 0.25 µM, [TO] = 0.5 µM for 22AG and TBA, 0.75 µM for ds26, cacodylate buffer.*

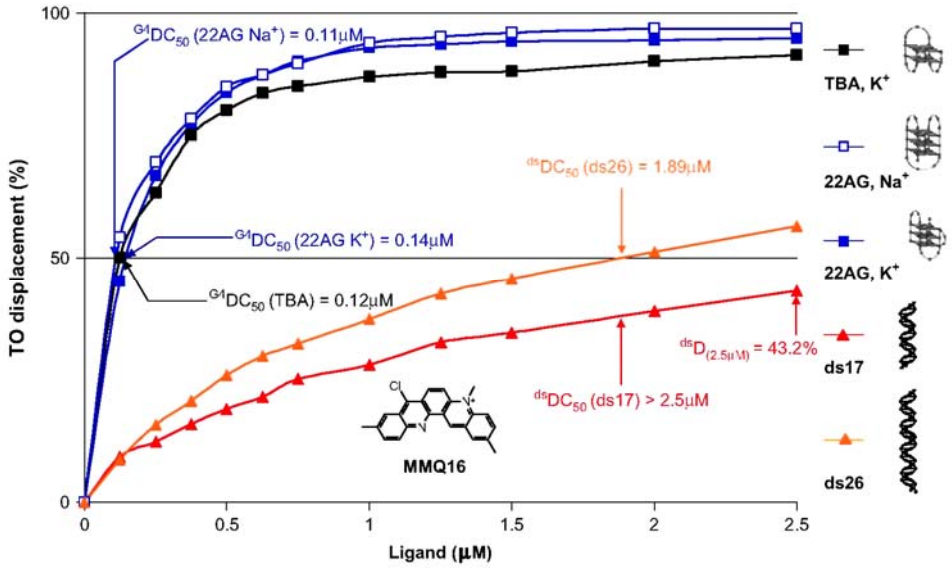

*Published in : Biochimie (2008), vol. 90, pp. 1207-1223*
*Status : Postprint (Author's version)*

***Fig. 6**. Diagrammatic bar representation of G4-FID mapping of the 16 studied ligands, i.e. G4-FID experiments performed with the duplex-DNAs dsl7 (red bar) and ds26 (orange bar) and the quadruplex-DNAs 22AG in $K^+$ (deep blue bar) or $Na^+$-rich buffer (light blue bar) and TBA (black bar).*

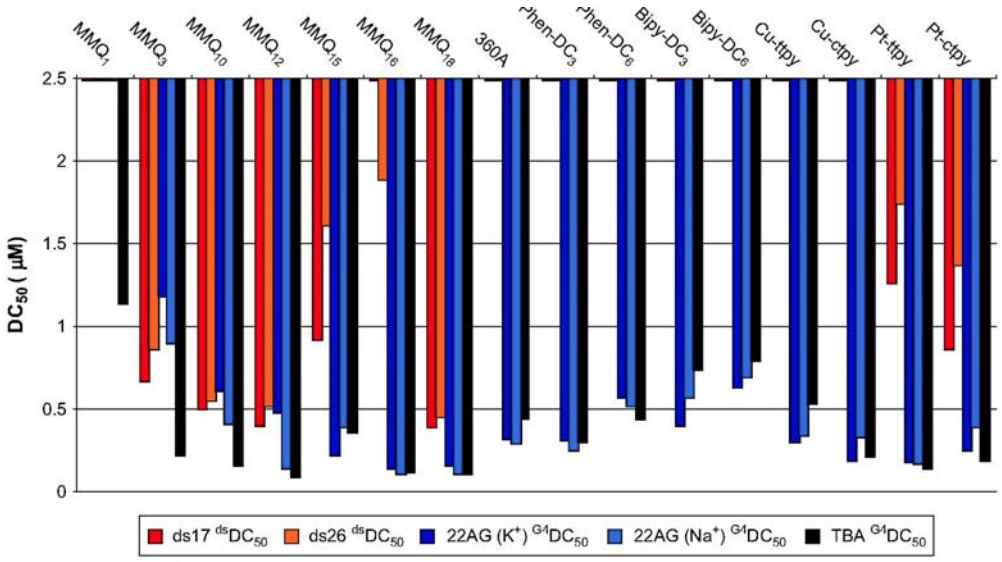


***Fig. 7**. Diagrammatic bar array representation of G4-FID selectivity of the 16 studied ligands, i.e. comparison of G4-FID experiments performed with 22AG $K^+$/ ds26 (red bars), 22AG $Na^+$/ds26 (orange bars), TBA/ds26 (yellow bars), 22AG $K^+$/dsl7 (deep blue bars), 22AG $Na^+$/dsl7 (light blue bars) and TBA/ds17 (green bars).*

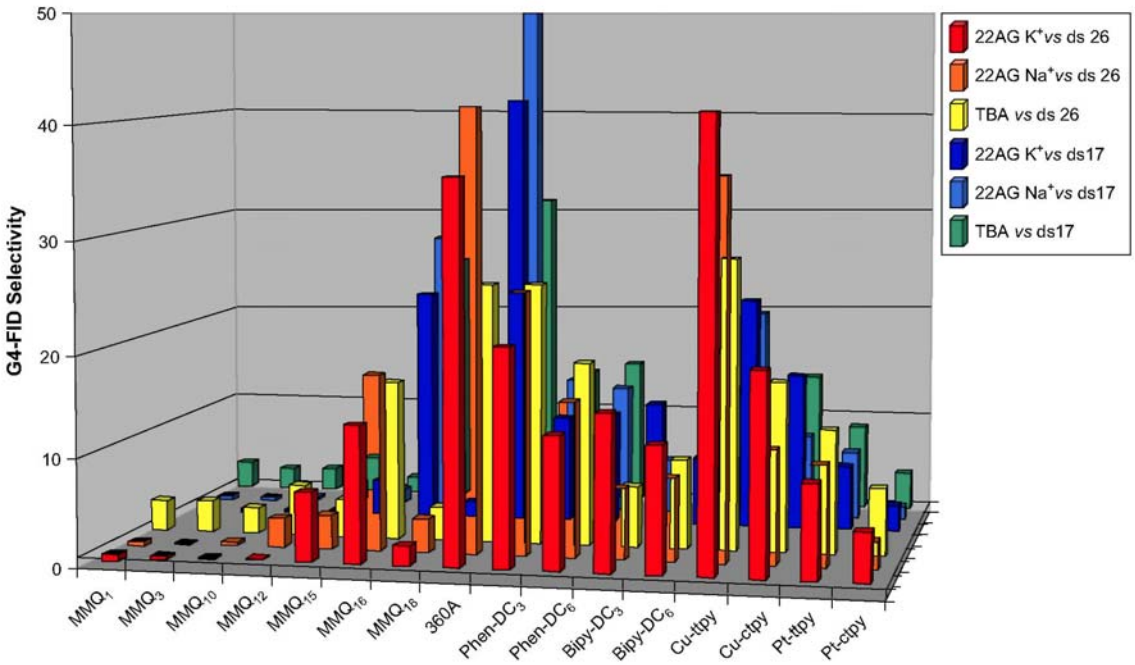

***Fig. 8.*** *Diagrammatic bar representation of FRET-melting results ($\Delta T_{1/2}$) obtained with F21T (0.2 µM) and the 16 studied ligands (1 µM) in 10 mM lithium cacodylate (pH 7.2) with 100 mM NaCl, in absence (dark green bars) or presence of competitive duplex-DNA ds26 (3 µM (light green bars) and 10 µM (light blue bars)) Values are given with a ± 1 °C precision.*

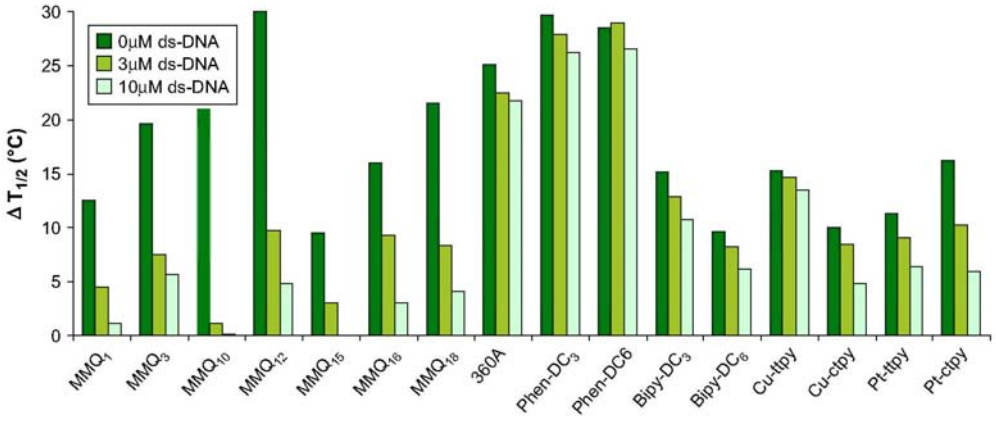


***Fig. 9****. ESI-MS profile of the association of $MMQ_{18}$ (A,B) and $MMQ_{16}$ (C,D) with Telo4 (A,C) and dsl2 (B,D), obtained with 5 µM of DNA and 10 µM of ligand, in 150 mM ammonium acetate, 15% MeOH.*

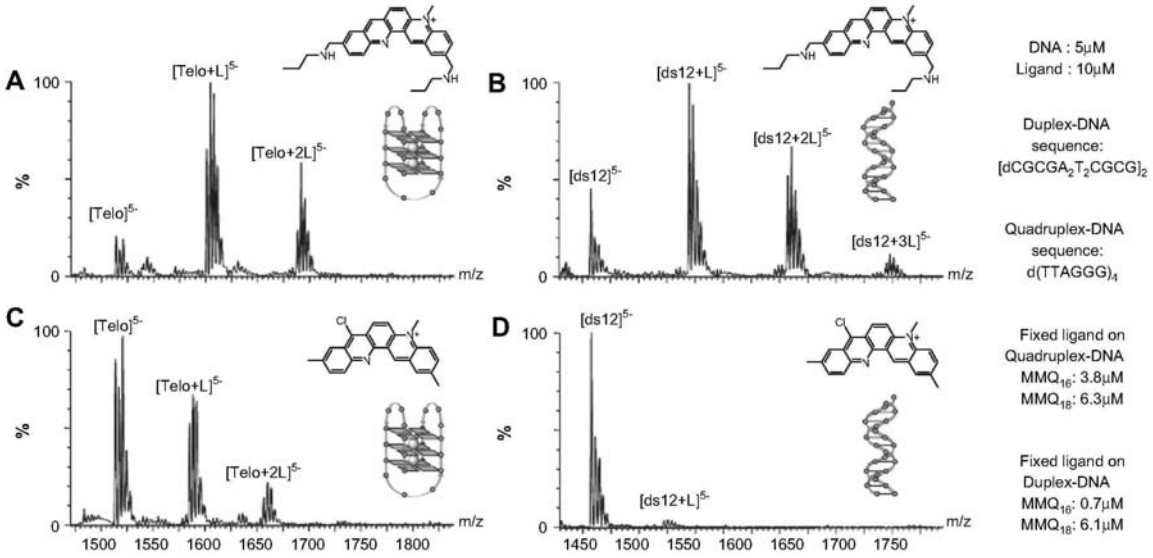


*3.5. G4-FID results of bisquinolinium dicarboxamide derivatives (360A, Phen-$DC_3$, Phen-$DC_6$, Bipy-$DC_3$ and Bipy-$DC_6$)*

Among the recent reported examples of G-quadruplex ligands, the bisquinolinium dicarboxamides derivatives **(360A, Phen-DC, Bipy-DC,** Fig. 4) appear among the most efficient and selective ones [41-46]. Herein, the G4-FID assay underlines the good TO-displacement ability from quadruplex-DNA of 360A ($^{G4}DC_{50}$ down to 0.29 µM, Table 3, Fig. 6), **Phen-$DC_3$** ($^{G4}DC_{50}$ down to 0.25 µM, Table 3, Fig. 6) and **Phen-$DC_6$** ($^{G4}DC_{50}$ down to 0.44 µM, Table 3, Fig. 6), while more modest results are obtained with **Bipy-$DC_3$** and **Bipy-$DC_6$** ($^{G4}$DCso up to 0.79 µM, Table 3, Fig. 6). Very interestingly, none of these compounds was able to reach the 50% threshold with duplex-DNA, evidencing a low duplex binding and hence a high degree of selectivity of the series (Table 3 and Fig. 7). **360A, Phen-$DC_3$** and **Phen-$DC_6$** appear as the most selective candidates (Est. Sel. between 11 and 50,

Table 3, Fig. 7) while less conclusive results are obtained with **Bipy-DC$_3$** and **Bipy-DC$_6$** (Est. Sel. between 5 and 15, Table 3, Fig. 7).

It should be noted that these results fully parallel those obtained by FRET-melting both in terms of affinity and selectivity (Table 3, Fig. 8) [45]. Indeed, while 360A is characterized by a $\Delta T_{1/2}$ of 25 °C, **Phen-DC** derivatives reached values close to 30°C ($\Delta T_{1/2}$ = 29.7°C for **Phen-DC$_3$** and 28.5 **°C** for **Phen-DC$_6$).** Interestingly, these thermal stabilizations were only poorly affected by the presence of competitive duplex-DNA (Table 3, Fig. 8). The structural rigidity of the central aromatic part of the ligand (pyridine for 360A, phenan-throline for **Phen-DC** and bipyridine for **Bipy-DC)** was demonstrated as pivotal for quadruplex-recognition: **Bipy-DC** derivatives were shown to be less potent particularly in terms of affinity ($\Delta T_{1/2}$ = 15.2 and 9.6°C for **Bipy-DC$_3$** and **Bipy-DCβ** respectively, Table 3) but also, to a somewhat lesser extent, in terms of selectivity (Table 3). These results are thus supported by both methods.

ESI-MS experiments confirm the results obtained with **Phen-DC$_3$** and **Phen-DC$_6$.** As for **MMQ$_{16}$** and **MMQ$_{18}$,** their associations were studied with the quadruplex-DNA Telo4 and the duplex-DNA ds12. As seen in Fig. 10A and C, the ESI-MS analysis allows determining a preferential 1:1 binding mode for both ligands. Additionally, these results underlined a better fixation of **Phen-DC$_3$** (4.9 µM) as compared to **Phen-DC$_6$** (3.8 µM), both ligands being characterized by a very high affinity for their quadruplex target. Interestingly, when the same experiments are carried out with duplex-DNA, marginal (0.1 µM) and no fixations were observed for **Phen-DC$_3$** and **Phen-DC$_6$** respectively, which corresponds to a high degree of selectivity for both ligands, these results being again fully reminiscent of what has been observed with G4-FID and FRET-melting.

***Fig. 10**. ESI-MS profile of the association of **Phen-DC$_3$ (A,B)** and **Phen-DC$_6$** (C,D) with Telo 4 (A,C) and dsl2 (B,D) obtained with 5 µM of DNA and 5 µM of ligand, in 150 mM ammonium acetate, 15% MeOH.*

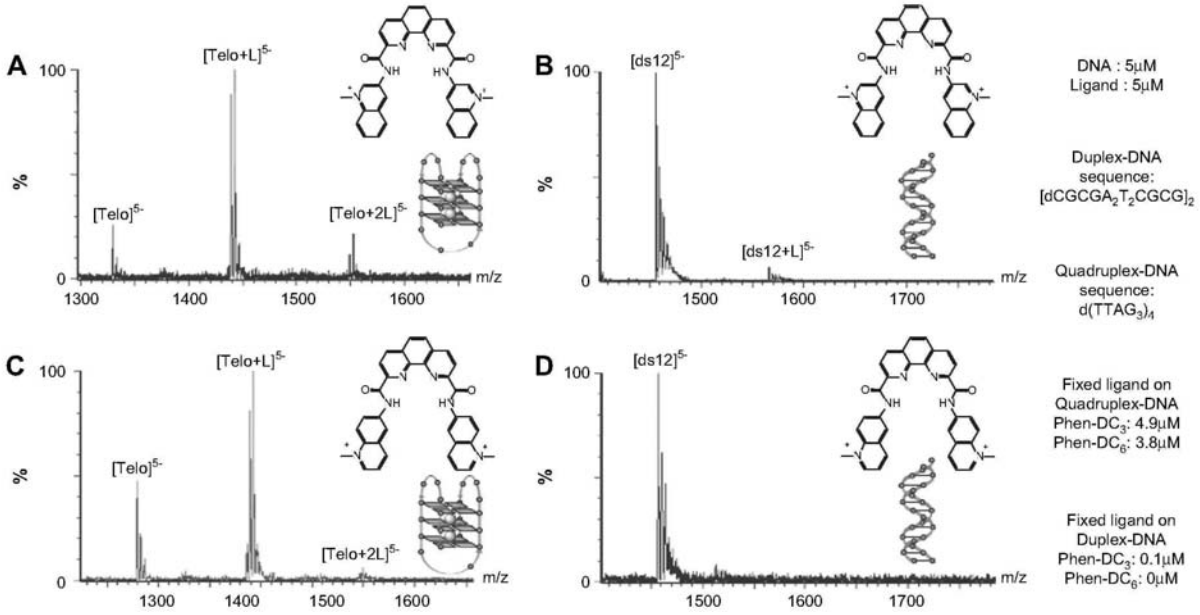


*3.6. G4-FID results of metallo-organic ligands (Pt-ttpy, Pt-ctpy, Cu-ttpy and Cu-ctpy)*

Metallo-organic ligands have been recently reported to be potent G-quadruplex binders [47-64]. Among them, the family of terpyridine metallo-organic complexes **(Pt-ttpy, Pt-ctpy, Cu-ttpy** and **Cu-ctpy,** Fig. 4) combines easy synthetic access and a good affinity/selectivity ratio for quadruplex-DNA [47]. The interest in this series resides in its ability to discriminate quadruplex- from duplex-DNA thanks to the geometry of the metal center, which can give novel guidelines for further design of selective ligands [47]. Through the present assay, and as already reported, all the complexes appear to be good to strong quadruplex binders (0.14 µM < $^{G4}DC_{50}$ < 0.53 µM, Table 4, Fig. 6), the platinum complex **Pt-ttpy** being the most efficient derivative (0.14 < $^{G4}DC_{50}$ < 0.18 µM, Table 4, Fig. 6). Notably, the TO displacement efficiency of the series is poorly affected by the structure of the quadruplex matrix (TBA vs. 22AG, Table 4, Fig. 6). In contrast, striking differences in their ability to bind duplex-DNA were shown: while the Pt complexes **Pt-tpy** and **Pt-ctpy** do associate with the two duplex-DNA

targets with a good affinity (0.86 μM<$^{ds}DG_{50}$< 1.92 μM, Table 4, Fig. 6) the Cu complexes appear very poorly active ($^{ds}$DGso > 2.5 μM in all cases, Table 4, Fig. 7).

As already pointed out, this divergence may originate in the geometry of the complexes, square planar for Pt(II) complexes and pyramidal for Cu(II) complexes, that favors intercalation between base pairs in the case of Pt complexes, whereas such a binding mode is impeded by the presence of an apical group for Cu complexes [47]. The FRET-melting assay confirmed the strong quadruplex-binding potential of the series (Table 4, Fig. 8) but also the better quadruplex- over duplex-DNA selectivity of Cu complexes as compared to Pt ones (Table 4, Fig. 8).

**4. Discussion**

Pharmacological targeting of quadruplex-DNA is currently emerging as a novel and very promising anti-cancer strategy and in this respect the development of methods devoted to the detection of small molecules able to interact strongly and selectively with this particular form of DNA is of crucial interest. Among the numerous already existing methods to monitor DNA-ligand interactions, four have been more particularly adapted to the quadruplex DNA field: FRET-melting assay, SPR technology, competitive dialysis, and ESI-MS. Each of these methods displays advantages and limitations that will be briefly examined herein and compared with the present G4-FID assay.

FRET-melting is based on the use of a quadruplex-forming oligonucleotide doubly-labeled with a pair of FRET donor and acceptor (usually *FAM:* 6-carboxyfluorescein and *Tamra:* 6-carboxy-tetramethylrhodamine) that allows to monitor the melting of the quadruplex via a FRET (fluorescence resonance energy transfer) effect [16,17]. Semi-quantitative evaluation of ligand binding affinity is obtained by measuring the increase in melting temperature induced by the ligand ($\Delta T_{1/2}$)· The quadruplex- over duplex-DNA selectivity is established via competitive FRET-melting which is carried out in presence of competitive duplex-DNA. This method is rapid and convenient; it has been adapted for high-throughput screening and used for an overwhelming majority of recently reported quadruplex-ligands. However, requisite for modified oligonu-cleotides, and possible interferences between ligands and the fluorescent labels represent the two main limitations of FRET-melting.

Biosensor-surface plasmon resonance (SPR) allows the quantitative analysis of small-molecule binding with surface-immobilized oligonucleotides via variations of refractive index [18-20]. In addition to its remarkable sensitivity, the unique feature of the SPR technique is that it enables the determination of both thermodynamic (equilibrium constant, Gibbs energy of binding, stoichiometry) and kinetic *($k_{on}/k_{off}$)* parameters of the interaction. The quadruplex- over duplex-DNA selectivity is inferred from the binding affinity values determined for each structure. However, because SPR method relies on a system in which a lot of parameters have to be carefully controlled (chip selection, probe immobilization, ionic strength solution, temperature, buffer component, etc.), great care has to be taken in the analysis of collected data.

Electrospray mass spectrometry (ESI-MS) has emerged as a powerful technique to select lead compounds on the basis of non-covalent ligand-DNA interactions ([21-24,38] and companion article from Rosu et al. in this issue). The direct readout of the stoichiometries of all complexes formed, including minor species, is a very attractive characteristic of ESI-MS analysis. The quantification of the free and bound DNA species allows direct determination of the amount of bound ligand and of equilibrium binding constants, and hence determination of selectivity by comparison of different targets. ESI-MS does not require modified oligonucleotides and allows using a broad variety of duplex- and quadruplex-DNAs. However, an inherent characteristic of electrospray is its incompatibility with the presence of alkaline salts in the sample, and the necessity to replace NaCl or KC1 by ammonium acetate. This leads to two limitations: (1) special oligonucleotide desalting procedures must be applied for the analysis of DNA structures larger than 50 bases, and (2) in some cases the structure of highly polymorphic G-quadruplexes can be different in ammonium acetate than in NaCl or KC1. Finally, ESI-MS as well as SPR require specific know-how and relatively expensive equipments.

Competition dialysis also allows the analysis of the association of a small molecule with greatly expanded array of nucleic acid forms (from single-stranded to duplex-, triplex-and quadruplex-DNA of various natures) in a quasi-unlimited manner [27-29]. This highly comparative assay is based on the equilibrium association of a putative ligand when dia-lyzed against a selected panel of DNA structures, and provides direct access to quantitative parameters of the association. Now adapted as a high-throughput screening, this protocol only suffers from the time-consuming preparation of nucleic acid stocks, as well as its marked dependence on spectroscopic properties (fluorescence, UV/Vis absorbance) of the ligand.

In this context, our goal in adapting the well-known FID technology to G-quadruplex ligand detection was to combine several advantages of the previously depicted methods in an easy to implement screening assay. The G4-FID assay presented herein is based on the competitive displacement of thiazole orange fluorescent probe from various DNA-matrices (quadruplex- and duplex-DNA) by increasing amounts of the ligand subjected to evaluation. Hence it will suffer from the major drawback of the FID methodology, i.e. the possible indirect competition when the binding site of the ligand and that of the probe are different. In the present case, this is also combined with the intrinsic polymorphism of quadruplex-DNA, which could lead eventually to mixtures of complexes. Additionally, though a broad diversity of compounds can be evaluated via the G4-FID assay (Fig. 4), another limitation lies in the absorption characteristics of the studied molecule that should not overlap neither with the absorption nor with the emission spectra of the probe to avoid filtering and re-absorption effects. For instance the well-known ligand **TMPyP4** [3,5,15] could not be properly evaluated since it presents a significant absorbance between 480 and 540 nm ($\varepsilon_{501nm}$ = 19,200 $M^{-1}$ $cm^{-1}$ ) leading to a biased fluorescence decrease. Finally, like for FRET-melting assay, the study of ligand-quadruplex association is limited to semi-quantitative analysis. However, the main advantages of G4-FID are (1) the use of unmodified oligonucleotides, which opens the possibility of being performed with a broad variety of DNA matrices (like equilibrium dialysis or ESI-MS), (2) the possibility to study DNA-ligand interaction in physiological conditions in terms of temperature (unlike FRET-melting assay) or cationic environment (unlike ESI-MS), and (3) the amenability to a high-throughput screening assay, like FRET-melting or competition dialysis assays.

To test the robustness of our protocol, the influence of several key parameters (DNA matrix, salt conditions) was investigated in depth. Initially the G4-FID assay was designed with 22AG, one of the most studied quadruplex-forming oligonucleotides (QFO) mimicking the human telomeric repeat, and a short 17 bp duplex-DNA (ds17). We exploited the convenient adaptability of this assay to evaluate the impact of the nature of each DNA-matrix (quadruplex- and duplex-DNA) on the G4-FID data reproducibility. For that purpose, TBA, a QFO not subjected to polymorphism [34,35,65], and a longer 26 bp-duplex DNA (ds26) were used. These assays were then performed with a representative panel of 16 fully characterized quadruplex ligands (Fig. 4), differing by their nature, from small organic molecules to metallo-organic complexes, and thus likely to interact with quadruplex-DNA via various modes, from PIr-stacking to random electrostatic interactions. For each quadruplex-ligand a set of G4-FID experiments have then been performed, with 2 quadruplex structures (22AG in $K^+$ or $Na^+$ solution and TBA) and 2 DNA duplexes (ds17 and ds26), thus offering a global "mapping" of its interaction with the various DNA forms.

Globally, within each series, results obtained with 22AG $K^+$, $Na^+$ or TBA confirm the trends of the FRET-melting ones, thus supporting the reliability of the G4-FID assay. In terms of quadruplex affinity, several conclusions can be drawn: firstly, the displacement of TO is easier from TBA (a quadruplex-DNA selected for its absence of polymorphism) than from 22AG ($^{G4}DC_{50}$ values are ~9% (mean value) lower with TBA, in $K^+$ conditions). This observation could indicate a slight difference in the binding affinity of TO to each quadruplex (i.e. lower for TBA), which was not evidenced by fluorescence titration but pointed out by ESI-MS analysis. In both cases a less drastic competition will result, thereby leading to a more accurate evaluation of the affinity of a given ligand. Alternatively this can originate in a higher similarity of binding site/mode for TO and the studied ligand in the case of TBA (direct vs. indirect competition). This is illustrated by **$MMQ_1$,** which cannot be evaluated by the use of 22AG in $K^+$ or $Na^+$ solution, despite a fair quadruplex stabilization ($\Delta T_{1/2}$ = 12 °C) and its fully characterized interaction with external quartet of quadruplex DNA [25,39]. Although this concerns only one ligand over the 16 evaluated, obtained results pinpoint the limit of the method: ligands that are thought to interact with quadruplex-DNA via a unique binding mode (π-stacking on the external tetrad) will compete directly with the probe whereas those that may interact via mixed binding modes (π-stacking and electrostatic interactions) will compete indirectly, and thus will be more subjected to underestimation of their performances. This is reflected by the variations of $DC_{50}$ values that is small ($\Delta[^{G4}DC50] < 0.2$ µM) for most series (*N*-methylated quinacridine, Phen-DC derivatives, metallo-organic complexes), whereas the polyammonium ligands (e.g. **$MMQ_1$** and to a lesser extent **$MMQ_3$)** are characterized by $\Delta[^{G4}DC_{50}] > 0.2$ µM. However, in the three cases (22AG $K^+$, $Na^+$ and TBA), and although $^{G4}DC_{50}$ values are subjected to some error (± 10-20%), a very good agreement was observed between $^{G4}DC_{50}$ and data obtained by FRET-melting: globally the lowest determined $^{G4}DC_{50}$ values correspond to the highest $\Delta T_{1/2}$ values since all compounds with $\Delta T_{1/2} > 16$ °C are characterized by $DC_{50} < 0.44$ µM. This observation led us to define an 'efficiency threshold' (Fig. 11), i.e. an arbitrary value ($^{G4}DC_{50}$ = 0.5 µM) above which the ligand is not considered a good candidate for quadruplex targeting. This only concerns three molecules here, namely **$MMQ_1$, Bipy-$DC_3$** and **Bipy-$DC_6$.**

In terms of selectivity, only few discrepancies were observed when the selectivity was measured with TBA or 22AG vs. ds17 or ds26 (Figs. 6 and 7). Indeed, irrespective of the quadruplex/duplex combination, higher selectivity values correlate with the most robust ligands as judged by competitive FRET-melting assay: for

example, all compounds with selectivity values >10 are characterized by a good resistance of the stabilization in the presence of competitive ds26. More precisely, the most selective ligands detected through G4-FID assay **(360A, Phen-DC$_3$, Phen-DC$_6$** and **Cu-ttpy** with selectivity values of 25, 25, 18, and 28 respectively, Tables 1-4) are the most selective via FRET-melting assay: the ligand induced stabilization is strongly maintained in presence of 15-fold excess of ds26 as compared to the stabilization without competitive duplex-DNA (90%, 94%, 100% and 95% for **360A, Phen-DC$_3$, Phen-DC$_6$** and **Cu-ttpy,** respectively, Tables 1-4). It is worth noting that, for some ligands, the selectivity evaluated by G4-FID was fully confirmed by ESI-MS analysis (Figs. 9 and 10). Altogether these observations led us to define an arbitrary "selectivity threshold" i.e. an arbitrary Sel. value =10 (Fig. 12), above which the ligand is considered as selective for quadruplex- over ds26 duplex-DNA. This concerns seven molecules here, namely **MMQ$_{16}$, 360A, Phen-DC$_3$, Phen-DC$_6$, Cu-ttpy, Cu-ctpy** and **Pt-ttpy.**

In conclusion, our initial aim was to develop a fluorimetric assay for affinity ranking of putative quadruplex ligands, which would be conveniently applicable in every laboratory. The promising G4-FID assay has been fully investigated herein, and its convenience and reliability validated by the study of 16 fully characterized G-quadruplex ligands. The robustness of the protocol allows the use of different DNA-matrices (both duplex- and quadruplex-DNA), in different cationic (salt) conditions. Concerning quadruplex-DNA, noticeable differences have been pinpointed in using 22AG in $K^+$ or $Na^+$-solutions (the TO-displacement being easier in presence of $K^+$), and TBA (the TO-displacement is easier from TBA than from 22AG). These observations can be interpreted on the basis of their structural divergences, knowing that 22AG is characterized by two lateral and one diagonal loops under its $Na^+$-favored form [1,32,33,66], two lateral and one double-chain reversal loops under its $K^+$-favored form [1,32,33,67-70], while TBA presents three lateral loops [1,32-35]. However, further interpretations of these observations seem difficult, since these structural differences are themselves a matter of heated controversy in the current literature.

Most importantly, the results as a whole allow concluding that the FID test is applicable with reliability to various quadruplex matrices. Concerning duplex-DNA, we were pleased to observe that comparable results were obtained with ds17 and ds26, with some minor discrepancies, underlining the fact that the present G4-FID assay is not purely electrostatically controlled. Additionally, the use of two duplex-DNAs of clearly different natures validates the present assay, since it provides a control that insures that the system is not biased via specific TO interaction with one or the other duplex-DNA. Altogether, the collected data highlight that TBA, 22AG, ds17 and ds26 are valuable G4-FID partners for the detection of ligands with high affinity (the affinity threshold value being $^{G4}DC_{50} < 0.5$ µM) and quadruplex-over duplex-DNA selectivity (the selectivity threshold value being Sel. > 10). Efforts are now being made to further extend the G4-FID assay to other quadruplex-forming sequences of biological interest (i.e. oncogene sequences) and to investigate implementation to 96-well plates for high-throughput screening of quadruplex ligands.

***Fig. 11**. Diagrammatic bar representation of G4-FID results of the 16 studied ligands with TBA as quadruplex-DNA matrix.*

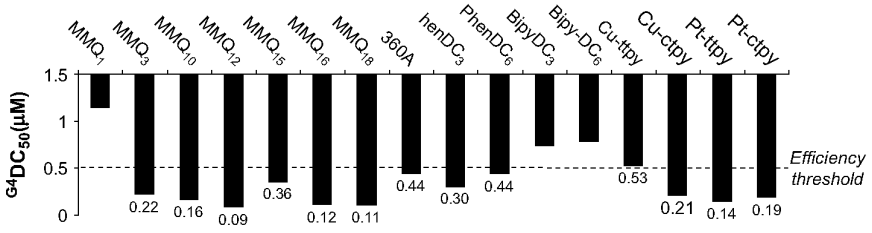

***Fig. 12**. Diagrammatic bar representation of G4-FID selectivity of the 16 studied ligands for G4-FID experiments performed with TBA/ds26.*

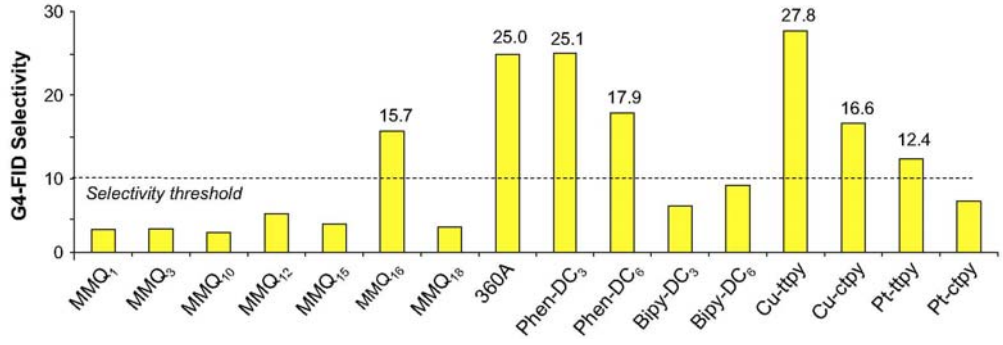


**Acknowledgments**

We would like to deeply thank our daily collaborators for their synthetic work (in particular Candide Hounsou, Elsa De Lemos), and Dr. Sophie Bombard for her scientific support. The *Centre National de la Recherche Scientifique* (CNRS) and *Commissariat a l'Energie Atomique* (CEA) are also gratefully acknowledged for their financial support (C.A., H.B.). Financial support from the *Fonds de la Recherche Scientifi-que-FNRS* (Belgium) is also acknowledged (FRFC grant 2.4.623.05, FRIA doctoral fellowship to N.S., post-doctoral fellowship to F.R., and research associate position to V.G). M.P.T.F. and V.G. also thank the "Tournesol program (CGRI-FNRS-CNRS) for bilateral France-Belgium collaborations". J.-L.M. and A.D.C. thank the European FP6 "MolCancerMed" program (LSHC-CT-2004-502943) for financial support.

**Appendix A. Supplementary data**

Supplementary data associated with this article can be found, in the online version, at doi: 10.1016/j.biochi.2008.02.019.

**References**

[1] S. Neidle, S. Balasubramanian, Quadruplex Nucleic Acid, RSC Publishing, Cambridge, 2006, 301.

[2] D.J. Patel, A.T. Phan, V. Kuryavyi, Human telomere, oncogenic promoter and 5'-UTR G-quadruplexes: diverse higher order DNA and RNA targets for cancer therapeutics, Nucleic Acids Res. 35 (2007) 7429-7455.

[3] B. Pagano, C. Giancola, Energetics of quadruplex-drug recognition in anticancer therapy, Current Cancer Drug Targets 7 (2007) 520-540.

[4] J.T.Davis, G-quartets 40 years later: from 5'-GMP to molecular biology and supramolecular chemistry, Angew. Chem. Int. Ed. 43 (2004) 668-698.

[5] D. Monchaud, M.-P Teulade-Fichou, A hitchhiker's guide to G-quadruplex ligands, Org. Biomol. Chem. 6 (2008) 627-636.

[6] L.H. Hurley, DNA and its associated processes as targets for cancer therapy, Nature Reviews Cancer 2 (2002) 188-200.

[7] S. Neidle, G Parkinson, Telomere maintenance as a target for anticancer drug discovery, Nature Reviews Drug Discovery 1 (2002) 383-393.

[8] J.-L. Mergny, J.-F Riou, P. Mailliet, M.-P. Teulade-Fichou, E. Gilson, Natural and Pharmacological regulation of telomerase, Nucleic Acids Res. 30 (2002) 839-865.

[9] E.M. Rezler, D.J. Bearss, L.H. Hurley, Telomere inhibition and telomere disruption as processes for drug targeting, Annu. Rev. Pharmacol. Toxicol. 43 (2003) 359-379.

[10] S. Neidle, D.E. Thurston, Chemical approaches to the discovery and development of cancer therapies, Nature Reviews Cancer 5 (2005) 285-296.

[11] L. Oganesian, T.M. Bryan, Physiological relevance of telomeric G-quadruplex formation: a potential drug target, BioEssays 29 (2007) 155-165.

[12] N. Maizels, Dynamic roles for G4 DNA in the biology of eukaryotic cells, Nat. Struct. Biol. 13 (2006) 1055-1059.

[13] M. Fry, Tetraplex DNA and its interacting proteins, Front. Biosci. 12 (2007) 4336-4351.

[14] L. Kelland, Targeting the limitless replicative potential of cancer: the telomerase/telomere pathway, Clin. Cancer Res. 13 (2007) 4960-4963.

[15] A. De Cian, L. Lacroix, C. Douarre, N. Temine-Smaali, C. Trentesaux, J.-F. Riou, J.-L. Mergny, Targeting telomeres and telomerase, Biochimie 90 (2008) 131-155.

[16] J.-L. Mergny, J.-C. Maurizot, Fluorescence resonance energy transfer as a probe for G-quartet formation by a telomeric repeat, ChemBioChem 2(2001) 124-132.

[17] A. De Cian, L. Guittat, M. Kaiser, B. Sacca, S. Amrane, A. Bourdoncle, P. Alberti, M.-P. Teulade-Fichou, L. Lacroix, J.-L. Mergny, Fluorescence-based melting assays for studying quadruplex ligands, Methods 42 (2007) 183-195.

[18] E.W. White, F. Tanious, M.A. Ismail, A.P Reszka, S. Neidle, D.W. Boykin, W.D. Wilson, Structure-specific recognition of quadruplex DNA by organic cations: influence of shape, substituents and charge, Biophys. Chem. 126 (2007) 140-153.

[19] B. Nguyen, FA. Tanious, W.D. Wilson, Biosensor-surface plasmon resonance: quantitative analysis of small molecule-nucleic acid interactions, Methods 42 (2007) 150-161.

[20] J.E. Redman, Surface plasmon resonance for probing quadruplex folding and interactions with proteins and small molecules, Methods 43 (2007) 302-312.

[21] V. Gabelica, E.S. Baker, M.-P. Teulade-Fichou, E. De Pauw, M.T. Bowers, Stabilization and structure of telomeric and c-myc region intramolecular G-quadruplexes: the role of central cations and small planar ligands, J. Am. Chem. Soc. 129 (2007) 895-904.

[22] L. Guittat, A. De Cian, F. Rosu, V. Gabelica, E. De Pauw, E. Delfourne, J.-L. Mergny, Ascididemin and meridine stabilise G-quadruplexes and inhibit telomerase in vivo, Biochim. Biophys. Acta 1724 (2005) 375-384.

[23] F. Rosu, V. Gabelica, K. Shin-ya, E. De Pauw, Telomestatin-induced stabilization of the human telomeric DNA quadruplex monitored by electrospray mass spectrometry, Chem. Commun. (2003) 2702—2703.

[24] C. Carrasco, F. Rosu, V. Gabelica, C. Houssier, E. De Pauw, C. Garbay-Jaureguiderty, B. Roques, W.D. Wilson, J.B. Chaires, M.J. Waring, C. Bailly, The binding of the antitumor drug ditercalinium to quadruplex DNA, ChemBioChem3 (2002) 1235-1241.

[25] J.-L. Mergny, L. Lacroix, M.-P. Teulade-Fichou, C. Hounsou, L. Guittat, M. Hoarau, P.B. Arimondo, J.-P Vigneron, J.-M. Lehn, J.-F Riou, T. Garestier, C. Helene, Telomerase inhibitors based on quadruplex ligands selected by a fluorescence assay, Proc. Natl. Acad. Sci. USA 98 (2001) 3062-3067.

[26] M.-P. Teulade-Fichou, C. Carrasco, L. Guittat, C. Bailly, P. Alberti, J.-L. Mergny, A. David, J.-M. Lehn, W.D. Wilson, Selective recognition of G-quadruplex telomeric DNA by a bis(quinacridine) macrocycle, J. Am. Chem. Soc. 125 (2003) 4732-4740.

[27] J. Ren, J.B. Chaires, Sequence and structural selectivity of nucleic acid binding ligands, Biochemistry 38 (1999) 16067-16075.

[28] PA. Ragazzon, N.C. Garbett, J.B. Chaires, Competition dialysis: a method for the study of structural selective nucleic acid binding, Methods 42 (2007) 173-182.

[29] PA. Ragazzon, J.B. Chaires, Use of competition dialysis in the discovery of G-quadruplex selective ligands, Methods 43 (2007) 313-323.

[30] Y. Yao, Q. Wang, Y.-H. Hao, Z. Tan, An exonuclease I hydrolysis assay for evaluating G-quadruplex stabilization by small molecules, Nucleic Acids Res. 35 (2007) e68.

[31] D. Monchaud, C. Allain, M.-P. Teulade-Fichou, Development of a fluorescent intercalator displacement assay (G4-FID) for establishing quadruplex-DNA affinity and selectivity of putative ligands, Bioorg. Med. Chem. Lett. 16 (2006) 4842-4845.

[32] S. Burge, G.N. Parkinson, P. Hazel, A.K. Todd, S. Neidle, Quadruplex DNA: sequence, topology and structure, Nucleic Acid Res. 34 (2006) 5402-5415.

[33] A.T. Phan, V. Kuryavyi, D.J. Patel, DNA architecture: from G to Z, Curr. Opin. Struct. Biol. 16 (2006) 288-298.

[34] R.F. Macaya, P. Schultze, F.W. Smith, J.A. Roe, J. Feigon, Thrombin-binding DNA aptamer forms a unimolecular quadruplex structure in solution, Proc. Natl. Acad. Sci. USA 90 (1993) 3745-3749.

[35] V.M. Marathias, PH. Bolton, Structure of the potassium-saturated, 2:1, and intermediate, 1:1, forms of a quadruplex DNA, Nucleic Acids Res. 28 (2000) 1969-1977.

[36] J. Nygren, N. Svanvik, M. Kubista, The interactions between the fluorescent dye thiazole orange and DNA, Biopolymers 46 (1998) 39-51.

[37] D.L. Boger, B.E. Fink, S.R. Brunette, WC. Tse, M.P Hedrick, A simple, high-resolution method for establishing DNA binding affinity and sequence selectivity, J. Am. Chem. Soc. 123 (2001) 5878-5891.

[38] F Rosu, V. Gabelica, C. Houssier, E. De Pauw, Determination of affinity, stoichiometry and sequence selectivity of minor groove binder complexes with double-stranded oligodeoxynucleotides by electrospray ionization mass spectrometry, Nucleic Acids Res. 30 (2002) e82.

[39] C. Hounsou, L. Guittat, D. Monchaud, M. Jourdan, N. Saettel, J.-L. Mergny, M.-P. Teulade-Fichou, G-quadruplex recognition by quinacridines: a SAR, NMR and biological study, ChemMedChem 2 (2007) 655-666.

[40] C. Allain, D. Monchaud, M.-P. Teulade-Fichou, FRET templated by G-quadruplex DNA: a specific ternary interaction using an original pair of donor/acceptor partners, J. Am. Chem. Soc. 128 (2006) 11890-11893.

[41] T. Lemarteleur, D. Gomez, R. Paterski, E. Mandine, P. Mailliet, J.-F. Riou, Stabilization of the c-myc gene promoter quadruplex by specific ligands' inhibitors of telomerase, Biochem. Biophys. Res. Commun. 323 (2004) 802-808.

[42] G. Pennarun, C. Granotier, L.R. Gauthier, D. Gomez, F. Hoffschir, E. Mandine, J.-F. Riou, J.-L. Mergny, P. Mailliet, FD. Boussin, Apopto-sis related to telomere instability and cell cycle alterations in human glioma cells treated by new highly selective G-quadruplex ligands, Oncogene 24 (2005) 2917-2928.

[43] C. Granotier, G. Pennarun, L. Riou, F. Hoffshir, L.R. Gauthier, A. De Cian, D. Gomez, E. Mandine, J.-F. Riou, J.-L. Mergny, P. Mailliet, B. Dutrillaux, FD. Boussin, Preferential binding of a G-quadruplex ligand to human chromosomes ends, Nucleic Acids Res. 33 (2005) 4182-4190.

[44] A. De Cian, J.-L. Mergny, Quadruplex ligands may act as molecular chaperones for tetramolecular quadruplex formation, Nucleic Acids Res. 35 (2007) 2483-2493.

[45] A. De Cian, E. DeLemos, J.-L. Mergny, M.-P. Teulade-Fichou, D. Monchaud, Highly efficient G-quadruplex recognition by bisquinolinium compounds, J. Am. Chem. Soc. 129 (2007) 1856-1857.

[46] A. De Cian, G. Cristofari, P. Reichenbach, E. De Lemos, D. Monchaud, M.-P. Teulade-Fichou, K. Shin-ya, L. Lacroix, J. Lingner, J.-L. Mergny, Reevaluation of telomerase inhibition by quadruplex ligands and their mechanisms of action, Proc. Natl. Acad. Sci. USA 104 (2007) 17347-17352.

[47] H. Bertrand, D. Monchaud, A. De Cian, R. Guillot, J.-L. Mergny, M.-P. Teulade-Fichou, The importance of the metal geometry in the recognition of G-quadruplex-DNA by metal-terpyridine complexes, Org. Biomol. Chem. 5 (2007) 2555-2559.

[48] C. Vialas, G. Pratviel, B. Meunier, Oxidative damage generated by an oxo-metalloporphyrin onto the human telomeric sequence, Biochemistry 39 (2000) 9514-9522.

[49] D.-F Shi, R.T. Wheelhouse, D. Sun, L.H. Hurley, Quadruplex-interactive agents as telomerase inhibitors: synthesis of porphyrins and structure-activity relationship for the inhibition of telomerase, J. Med. Chem. 44 (2001) 4509-4523.

[50] W. Tuntiwechapikul, J.T Lee, M. Salazar, Design and synthesis of the G-quadruplex-specific cleaving reagent perylene-EDTA.iron(II), J. Am. Chem. Soc. 123 (2001) 5606-5607.

[51] A. Maraval, S. Franco, C. Vialas, G. Pratviel, M.A. Blasco, B. Meunier, Porphyrin-aminoquinoline conjugates as telomerase inhibitors, Org. Biomol. Chem. 1 (2003) 921-927.

[52] L.R. Keating, V.A. Szalai, Parallel-stranded guanine quadruplex interactions with a copper cationic porphyrin, Biochemistry 43 (2004) 15891-15900.

[53] S.E. Evans, M.A. Mendez, K.B. Turner, L.R. Keating, R.T. Grimes, S. Melchior, V.A. Szalai, End-stacking of copper cationic porphyrins on parallel-stranded guanine quadruplexes, J. Biol. Inorg. Chem. 12 (2007) 1235-1249.

[54] S. Sato, H. Kondo, T. Nojima, S. Takenaka, Electrochemical telomerase assay with ferrocenylnaphthalene diimide as a tetraplex DNA-specific binder, Anal. Chem. 77 (2005) 7304-7309.

[55] I.M. Dixon, F. Lopez, J.-P. Esteve, A.M. Tejera, M.A. Blasco, G. Pratviel, B. Meunier, Porphyrin derivatives for telomere binding and telomerase inhibition, ChemBioChem 6 (2005) 123-132.

[56] J.E. Reed, A.A. Arnal, S. Neidle, R. Vilar, Stabilization of G-quadruplex DNA and inhibition of telomerase activity by square-planar nickel(II) complexes, J. Am. Chem. Soc. 128 (2006) 5992-5993.

[57] D.P.N. Goncalves, R. Rodriguez, S. Balasubramanian, J.K.M. Sanders, Tetramethylpyridinium porphyrazines—a new class of G-quadruplex inducing and stabilising ligands, Chem. Commun. (2006) 4685-4687.

[58] T. Ohyama, Y. Kato, H. Mita, Y Yamamoto, Exogenous ligand binding property of a heme-DNA coordination complex, Chem. Lett. 35 (2006) 126-127.

[59] C. Rajput, R. Rutkaite, L. Swanson, I. Haq, J.A. Thomas, Dinuclear monointercalating $Ru^{II}$ complexes that display high affinity binding to duplex and quadruplex DNA, Chem. Eur. J. 12 (2006) 4611-4619.

[60] I.M. Dixon, F Lopez, A.M. Tejera, J.-P. Esteve, M.A. Blasco, G. Pratviel, B. Meunier, A G-quadruplex ligand with 10000-fold selectivity over duplex DNA, J. Am. Chem. Soc. 129 (2007) 1502-1503.

[61] L. Ren, A. Zhang, J. Huang, P. Wang, X. Weng, L. Zhang, F. Liang, Z. Tan, X. Zhou, Quaternary ammonium zinc phthalocyanine: inhibiting telomerase by stabilizing G quadruplexes and inducing G-quad-ruplex structure transition and formation, ChemBioChem 8 (2007) 775-780.

[62] J.E. Reed, S. Neidle, R. Vilar, Stabilisation of human telomeric quadru-plex DNA and inhibition of telomerase by a platinum-phenanthroline complex, Chem. Commun. (2007) 4366-4368.

[63] H. Bertrand, S. Bombard, D. Monchaud, M.-P. Teulade-Fichou, A platinum-quinacridine hybrid as a G-quadruplex ligand, J. Biol. Inorg. Chem. 12 (2007) 1003-1014.

[64] R. Kieltyka, J. Fakhoury, N. Moitessier, M.F. Sleiman, Platinum phenanthroimidazole complexes as G-quadruplex DNA selective binders, Chem. Eur. J. 14 (2008) 1145-1154.

[65] M. Fialova, J. Kypr, M. Vorlickova, The thrombin binding aptamer GGTTGGTGTGGTTGG forms a bimolecular guanine tetraplex, Biochem. Biophys. Res. Commun. 344 (2006) 50-54.

[66] Y. Wang, D.J. Patel, Solution structure of the human telomeric repeat d[$AG_3(T_2AG_3)3$] G-tetraplex, Structure 1 (1993) 263-282.

[67] A. Ambrus, D. Chen, J. Dai, T. Bialis, R.A. Jones, D. Yang, Human telomeric sequence forms a hybrid-type intramolecular G-quadruplex structure with mixed parallel/anti-parallel strands in potassium solution, Nucleic Acids Res. 34 (2006) 2723-2735.

[68] J. Dai, C. Punchilhewa, A. Ambrus, D. Chen, R.A. Jones, D. Yang, Structure of the intramolecular human telomeric G-quadruplex in potassium solution: a novel adenine triple formation, Nucleic Acids Res. 35 (2007) 2440-2450.

[69] J. Dai, M. Carver, C. Punchilhewa, R.A. Jones, D. Yang, Structure of the hybrid-2 type intramolecular human telomeric G-quadruplex in $K^+$ solution: insights into structure polymorphism of the human telomeric sequence, Nucleic Acids Res. 35 (2007) 4927-4940.

[70] A.T Phan, V. Kuryavyi, K.N. Luu, D.J. Patel, Structure of two intramolecular G-quadruplexes formed by natural human telomere sequences in $K^+$ solution, Nucleic Acids Res. 35 (2007) 6517-6525.